ELSEVIER

Chemical Geology 191 (2002) 243–255

CHEMICAL GEOLOGY
INCLUDING
ISOTOPE GEOSCIENCE

www.elsevier.com/locate/chemgeo

Nondestructive chemical dating of young monazite using XRF 2. Context sensitive microanalysis and comparison with Th–Pb laser-ablation mass spectrometric data

Nadim C. Scherrer [a,*], Martin Engi [a], Alfons Berger [a], Randall R. Parrish [b], Andriy Cheburkin [c]

[a] *Institute of Geology University of Bern, Baltzerstrasse 1–3, CH-3012, Bern, Switzerland*
[b] *Department of Geology, University of Leicester and NERC Isotope Geosciences Laboratory, British Geological Survey, Keyworth, Notts NG12 5GG, UK*
[c] *Laurentian University, Ramsey Lake Rd., Sudbury, ON, Canada P3E 2C6*

Received 12 June 2001; received in revised form 19 November 2001; accepted 6 December 2001

Abstract

A newly developed XRF-microprobe at the Institute of Mineralogy and Petrology, University of Bern, Switzerland has been applied for precise chemical Th–U–Pb dating of individual monazite grains separated from Pb-free polished petrographic thin sections. The nondestructive nature of the XRF-measurement permitted a comparative study of dating methods by sequentially applying chemical dating by electron microprobe analysis (EMPA), chemical dating by XRF-microprobe analysis, and isotopic $^{208}Pb/^{232}Th$ dating by Laser Ablation Plasma Ionisation Multi-collector Mass Spectrometry (LA-PIMMS) analysis. As an example, the 2σ precision achieved with the XRF-microprobe for well characterised reference material, monazite FC-1 (TIMS age 54.3 ± 1 Ma; μ-XRF age 55.3 ± 2.6 Ma), doubly polished to 30 μm in thickness, is below 5% after 90 min integration time (50 kV; 30 mA) at a spatial resolution of 90 μm. At 38-μm spatial resolution, the uncertainty is 35% for the same integration time. The sample characteristics are 200–300 ppm of Pb (μ-XRF), 3.8–5.1 wt.% of Th (EMPA), and 0.4–1.4 wt.% U (EMPA). Combined with an electron microprobe and conventional optical microscopy, the XRF-microprobe is thus a competitive low-cost and nondestructive alternative to more costly isotopic methods. The XRF-microprobe is easy to use and maintain.

Keywords: Monazite; EMPA; XRF-microprobe; LA-PIMMS; Th–U–Pb dating

1. Introduction

Monazite is acclaimed to be one of the most promising accessory phases for dating metamorphism in amphibolite and higher grade granitic and pelitic rocks (Foster et al., 2000; Finger et al., 1998; Spear and Parrish, 1996). In rocks from polymetamorphic

* Corresponding author.
E-mail addresses: scherrer@geo.unibe.ch (N.C. Scherrer), engi@geo.unibe.ch (M. Engi), berger@geo.unibe.ch (A. Berger), rrp@nigl.nerc.ac.uk (R.R. Parrish), acheburkin@nickel.laurentian.ca (A. Cheburkin).

0009-2541/02/$ - see front matter
PII: S0009-2541(02)00159-6

terrains, often more than one population of monazite may be distinguished on the basis of textural relationships. For example, it has been observed that monazite inclusions within garnet preserve ages that are distinctly different from monazite ages found within the matrix (e.g., Foster et al., 2000; Montel et al., 2000; Simpson et al., 2000; Engi et al., 2001). This window to the past increases chances to time-constrain ancient geothermobarometric conditions of included assemblages, and thus may potentially permit dating of segments of the P–T paths.

Monazite rarely incorporates substantial amounts of common lead (Pb), and thus Pb_{total} is in most cases about equal to $Pb_{radiogenic}$. Since Th is a major element in monazite, sufficient $Pb_{radiogenic}$ is produced within 100–200 Ma such that Pb_{total} can be quantified by means of easily accessible electron microprobe analysis (Suzuki and Adachi, 1991a; Montel et al., 1996; Scherrer et al., 2000), offering the conventional petrologist a useful, albeit somewhat imprecise geochronometer (Suzuki and Adachi, 1991b; Montel et al., 1996; Rhede et al., 1996) with high spatial resolution (<5 μm). The fact that chemical age dating approximates isotopic dating in the case of monazite suggests that the lower limitation (minimum age) is set essentially by the analytical detection limit of the element Pb. The electron microprobe has clear limitations in dating geologically young samples due to significant background counts. The new XRF-microprobe technology achieves minimal background such that the detection limit of the XRF-microprobe instrument is as low as 10 ppm for Pb (Engi et al., this volume).

Aspects of sample preparation and full rare-earth element quantification of monazite (with particular emphasis on chemical Th–U–Pb dating) are described in Scherrer et al. (2000). Here, we present an alternative chemical dating method to acquire higher precision age information from monazite grains in thin section, utilising a newly developed XRF-microprobe. The instruments' precision and accuracy are evaluated against high precision isotopic dating by LA-PIMMS (Parrish et al., 1999), where $^{208}Pb/^{232}Th$ ratios corrected for ^{204}Pb are analysed. The comparison is based on sequential analysis of each grain by the different techniques.

Our aim was to retain the full context information of each single grain we attempted to date (cf. Engi et al., this volume). Doubly polished petrographic thin sections are perhaps the most versatile and informative method to characterise samples in petrology. Performing age dating of single grains in well-characterised thin sections is thus geologically far more powerful and informative than dating bulk mineral separates. This aspect becomes particularly important when dealing with polymetamorphic rocks, where multiple stages of monazite growth may have been preserved. A database combining quantitative chemical and isotopic data with visual textural information (optical and BSE) for each single grain provided a very useful tool to discern the meaning of each age analysis with respect to regional geology.

2. Chemical Th–U–Pb dating by XRF-microprobe

2.1. Instrument and technique

The original XRF-instrument and measurement techniques are described in Engi et al. (this volume) and Cheburkin et al. (1997). In short, the principal design elements of the energy-dispersive XRF-microprobe instrument are a conventional X-ray tube (Mo, fine focus, 3 kW), a focusing LiF monochromator, a sample holder (4-μm prolene), and an energy dispersive Si(Li) X-ray detector, cooled with liquid nitrogen. A pulse-processor converts the detected signal into a spectrum, which is processed on a computer. An optical microscope with a rotating x–y sample stage permits optical recognition and centering of the grain to be analysed prior to measurement. The system operates at normal room conditions (no vacuum). The main difference between previous versions and the newer instrument at the MPI Bern is the spherical (rather than cylindrical) LiF crystal used for X-ray beam focusing. This increases the intensity of the primary beam and reduces the beam shape to a circular spot. Integration time varies from 10 min to ~ 3 h and depends on the volume to be measured (choice of aperture, size of grain), and the amount of lead present (limiting factor). This, in turn, is a function of age (the older, the more Pb is present), and thorium and uranium contents. Currently, a maximum spatial resolution of ~ 38 μm (diameter) is achieved. Larger apertures (90–1000 μm) are available for better efficiency with homogenous grains, or

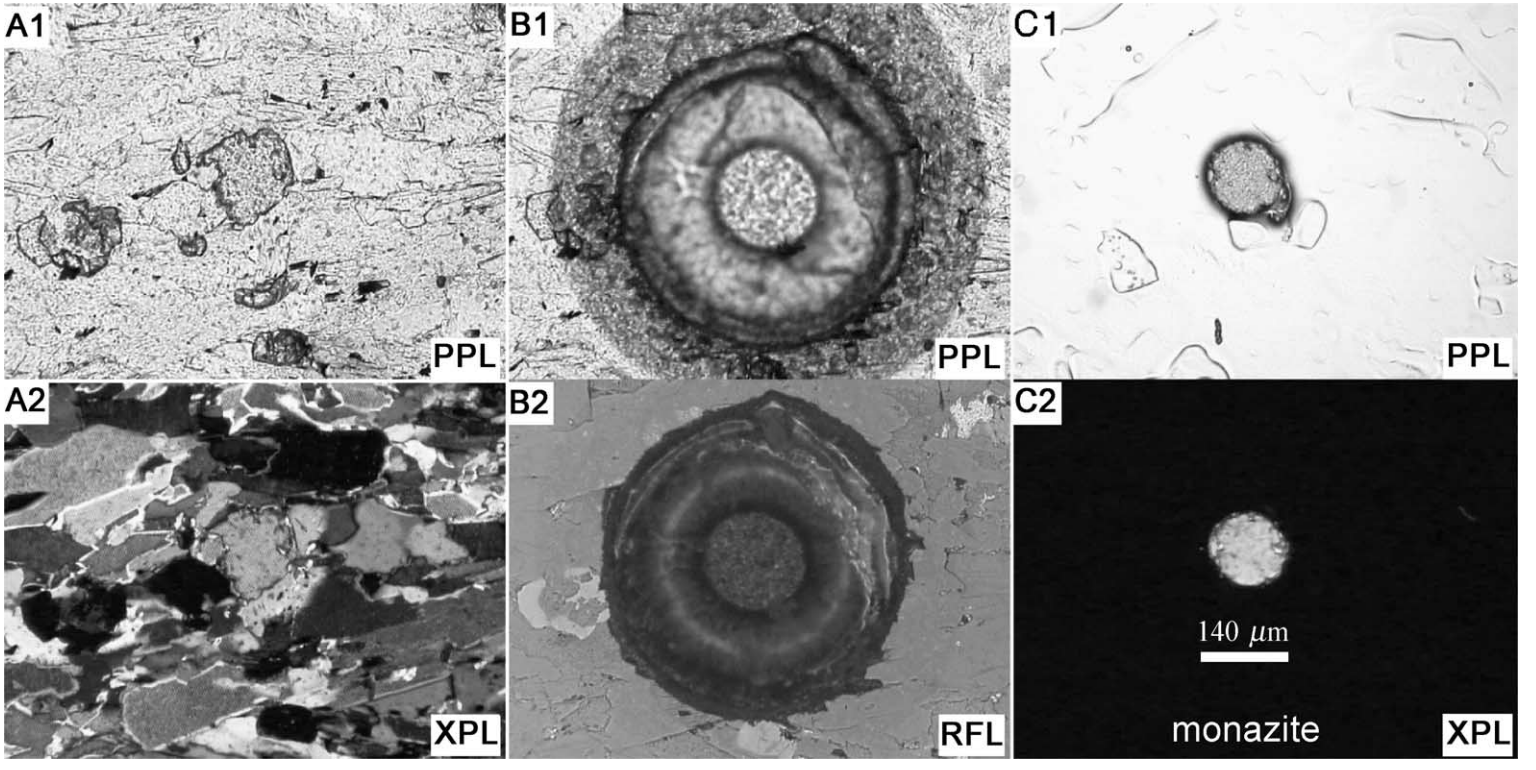

Fig. 1. (A) Optical image of a kyanite bearing garnet–mica gneiss with the view centered on a matrix monazite. (B) Optical images in transmitted and reflected light mode demonstrating the minimal loss of material at thin section scale by applying a micro diamond drill for the preparation of doubly polished grain mounts with full context control. The micro drill is mounted on a conventional optical microscope. The cloudy rim in the upper image is the zone of acetone leaching the glue of the thin section. (C) The finished grain mount ready for XRF-microprobe analysis. The substrate used is a 4-μm prolene foil, and the grains are mounted with Canada balsam. Canada balsam has several useful properties: it contains no common lead; it is nontoxic and easily dissolves and redissolves in alcohol; it is optically clear when dry. PPL = plane polarised light; XPL = crossed polarised light; RFL = reflected light.

Table 1
Electron microprobe data for the FC-1 monazite standard in element wt.% (average of nine analyses)

Method	EMP	TIMS
P	13.11	
Si	0.18	
Ca	0.90	
Y	2.48	
La	12.20	
Ce	23.24	
Pr	2.38	
Nd	8.70	
Sm	1.71	
Gd	1.39	
Tb	0.15	
Dy	0.71	
Ho	0.09	
Er	0.18	
Yb	0.01	
Pb	b.d.l.	0.02044
Th	4.63	
U	1.16	1.13502
O	27.55	
Total	100.78	
$^{208}Pb/^{232}Th$		0.002690

For comparison, the concentration of Pb and U analysed by TIMS were also included. Note that Pb contents are below the detection limit (b.d.l.) of the electron microprobe. Analytical settings are according to Scherrer et al. (2000).

different analytical requirements. Penetration depth of the X-ray beam is >30 μm. Thus, thick substrates such as mounting glass are not suitable for XRF-analysis for two reasons: (1) the thickness of a substrate causes dilution of the actual signal; (2) conventional mounting glass used in the preparation of petrographic thin sections may contain up to several ppm of Pb thus, causing unwanted interference. A further difference to the previous measurement technique (Engi et al., this volume) is the use of doubly polished, disk-shaped separates drilled from thin sections. This minimises topographic effects, which were encountered on analysing irregularly shaped whole grains derived from classical mineral separates. By using petrographic thin sections, rather than powdered rock as the starting sample material, thorough documentation of each grain in context prior to and complementing XRF-analysis is easy to achieve (quantitative analyses, BSE images of internal zonation and context, optical images) and leads to better control on the interpretation of age analysis on single grains.

2.2. Sample preparation for XRF-analysis

The preparation of lead-free polished thin sections, an essential precondition for chemical Th–U–Pb dating, is described in Scherrer et al. (2000). For reasons of limited visual control on the nondestructive and nonvisible beam, thin sections are prepared using an acetone-soluble glue so as to permit removal of doubly polished grains from the thin section by use of a diamond microdrill, acetone, and a preparation needle (Fig. 1). The separated grains are then mounted on a substrate producing minimal interference with the XRF signal (Fig. 1). A 4-μm thick prolene foil and Canada balsam offer easy handling with neither optical nor radiographic interference within the detection limit of the XRF-microprobe.

Since individual grains are removed from their original context for XRF-analysis, documentation should be as complete as possible, and thus, the following work is desirable prior to XRF sample preparation:

- Local context overview: BSE context image for each aggregate containing monazite.
- Internal chemical variation: BSE zonation image of each monazite grain.
- Quantitative analysis of monazite: for dating, Th contents of >1 wt.% are preferable. A chemical Th–U–Pb age by EMP may provide imprecise, but useful ‘reconnaissance’ information. Furthermore, complete quantitative analyses may provide

Table 2
Different age data of FC-1: XRF-measurements are compared to TIMS (Parrish, 1990, 1995) and LA-PIMMS (average of $n=16$) data

Technique	Age (Ma)	$\pm 2\sigma$	System	Comment
EMP	–		Th–U–Pb	Pb below detection limit
μ-XRF	55.3	2	Th–U–Pb	NOT corrected for ^{204}Pb
LA-PIMMS	54.4	1.5	$^{208}Pb/^{232}Th$	corrected for ^{204}Pb
	55.2	1.5	$^{208}Pb/^{232}Th$	NOT corrected for ^{204}Pb
TIMS	54.3	1	$^{208}Pb/^{232}Th$	corrected for ^{204}Pb
	56.3	1	$^{206}Pb/^{238}U$	corrected for ^{204}Pb

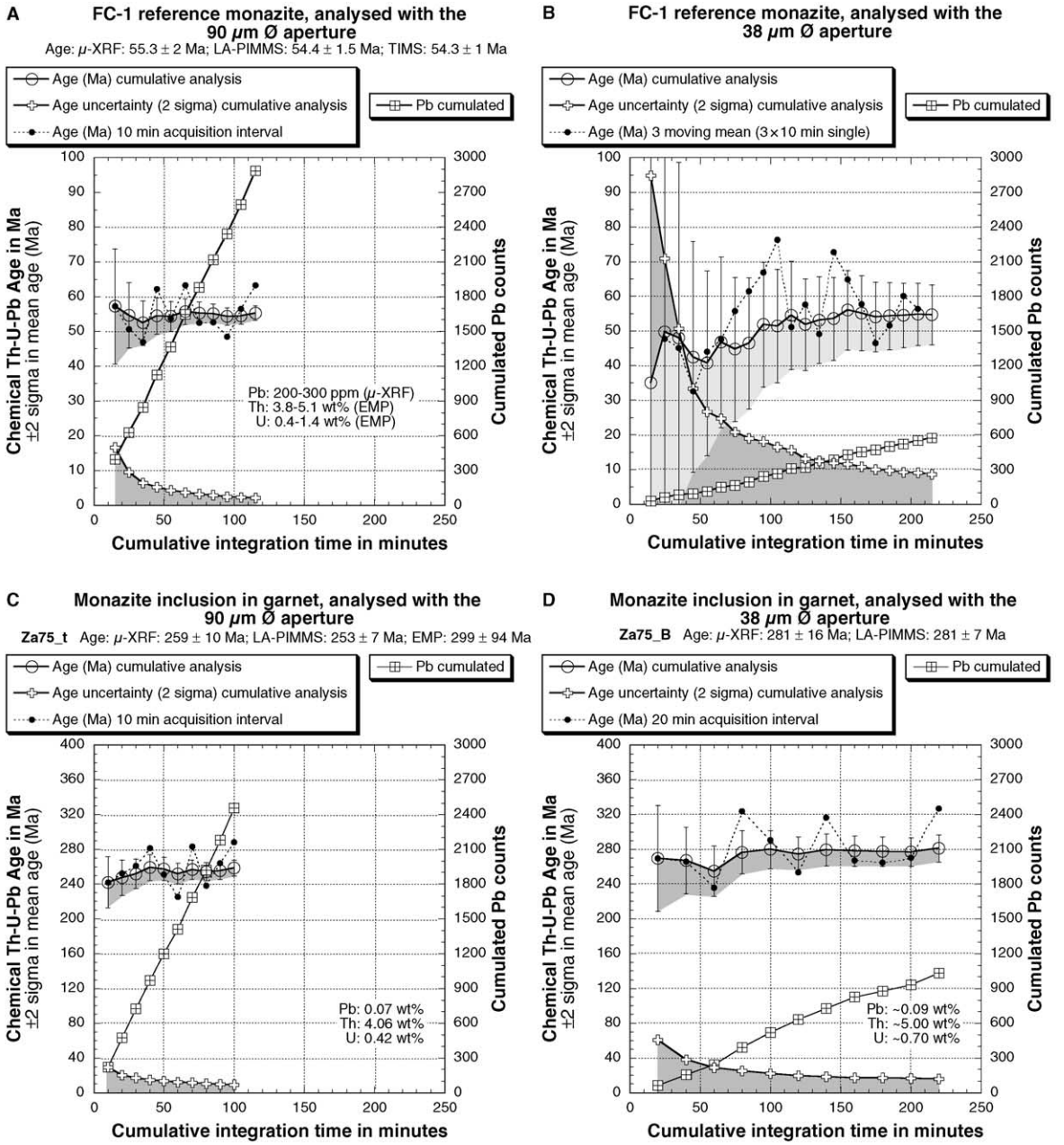

Fig. 2. These plots demonstrate the performance of the XRF-microprobe using two different spatial resolutions: 90 versus 38 μm, tested on reference material of Tertiary age, monazite FC-1 (A and B; see also Tables 1 and 2) and on two Permian monazite grains (C and D; Table 3). Instrument settings for Th–U–Pb age determination are commonly 30 kV at 50 nA. The plots are indicative of the integration time (*x*-axis) required and the uncertainties to be expected (shaded area) when analysing single monazite grains separated from thin sections (Fig. 1). The age uncertainties are based on the counting statistics of the Pb determination (shaded area). Note the implications for analysing small (< 50 μm on right) versus large (>90 μm on left) grains: with the small aperture, integration time is nine times longer to achieve similar counting statistics as with the 90-μm aperture (compare cumulated Pb counts of sample FC-1). Since the technique is nondestructive, analysis can be performed in cumulative mode and integration time can be adjusted individually until a satisfactory level of uncertainty is reached (within the limits of the technique). It is thus, possible to age date young grains smaller than 30 μm.

Table 3
Summary of age data presented in Fig. 3

Sample (Grain)		μ-XRF analysis							EMP analysis				
No.	Comment	Int. time (min)	Pb Lα (total counts)	± 2σ	Th Ll (total counts)	U Ll (total counts)	Th–U–Pb Age (Ma)	± 2σ (Ma)	ThO_2 (wt.%)	UO_2 (wt.%)	PbO (wt.%)	Th–U–Pb Age (Ma)	± 2σ (Ma)
1	99SL-145_1	60	33	20	27,758	693	42	23	n.a.	n.a.	n.a.	n.a.	n.a.
2	99SL145_g	60	34	38	9912	1084	101	101	0.426	0.046	b.d.	n.a.	n.a.
3	99SL145_v	60	19	22	19,650	919	33	34	2.487	0.228	b.d.	n.a.	n.a.
4	99SL145_v	60	19	22	19,650	919	33	34	2.487	0.228	b.d.	n.a.	n.a.
5	An91C_j	60	89	28	43,901	2364	67	19	4.997	0.437	b.d.	n.a.	n.a.
6	Bi9802b1	43	32	22	13,413	3089	56	35	n.a.	n.a.	n.a.	n.a.	n.a.
7	Mo9804_w	300	151	48	123,067	10,772	38	11	2.266	0.330	b.d.	n.a.	n.a.
8	Po73_e	120	109	50	89,956	13,603	33	14	n.a.	n.a.	n.a.	n.a.	n.a.
9	Po73_r	90	252	100	155,120	33,280	39	14	1.840	0.323	b.d.	n.a.	n.a.
10	To81_r	60	71	46	93,399	10,115	22	13	3.406	0.707	b.d.	n.a.	n.a.
11	Tr92a_d	240	243	92	161,218	8803	50	17	4.566	0.369	b.d.	n.a.	n.a.
12	Tr92_b	60	161	46	87,804	4847	61	16	4.109	0.312	b.d.	n.a.	n.a.
13	Tr92_f	60	194	42	131,695	12,975	44	9	10.246	1.224	0.026	43	52
14	Tr92_l	120	128	50	115,028	5674	37	13	3.571	0.316	b.d.	n.a.	n.a.
15	Tr92_m	60	101	38	65,832	6656	46	16	n.a.	n.a.	n.a.	n.a.	n.a.
16	Za75_j	60	84	28	44,385	6329	52	16	4.440	0.942	0.022	66	100
17	An91C_k in grt	60	633	60	52,310	4570	369	31	4.696	0.423	0.071	270	96
18	Pd79_l	30	652	126	91,692	646	263	46	n.a.	n.a.	n.a.	n.a.	n.a.
19	PD79_j	60	833	76	100,597	1781	298	24	5.351	0.105	0.045	184	100
20	PD79_n	30	283	64	34,717	1171	282	57	4.473	0.260	0.037	161	100
21	Ti81_g	60	738	84	79,059	6444	289	29	4.084	0.647	0.082	309	120
22	Za72_l	53	784	72	68,293	12,893	288	23	3.157	0.905	0.147	561	120
23	Za72_o	60	869	96	80,537	11,046	298	29	3.061	0.388	0.123	655	174
24	Za72_p	60	952	76	84,209	14,537	292	21	2.757	0.580	0.083	417	160
25	Za72_h	30	398	26	39,868	4245	293	34	3.263	0.724	0.099	413	132
26	Za75_h_zoned	20	445	78	64,078	5545	213	33	4.987	0.553	0.085	291	100
27	Za75_s in grt	40	468	90	47,187	4147	303	52	5.266	0.587	0.088	283	112
28	Za75_t in grt	100	2454	146	288,966	25,892	259	14	4.621	0.482	0.078	299	94
29	Za75_B in grt	220	1035	88	113,570	9461	281	21	n.a.	n.a.	n.a.	n.a.	n.a.
30	FC-1 std	75	1880	86	798,372	186,496	55	2	4.630	1.160	b.d.	n.a.	n.a.
31	G7 std	85	29,059	676	2,018,510	80,250	488	10	13.957	0.611	0.311	458	66
32	G1A std	25	39,311	886	2,625,514	12,672	554	11	12.973	0.187	0.310	535	78

Sample (Grain)		LA-PIMMS analysis																corr	
No.	Comment	^{208}Pb (V)	± 2σ	^{232}Th (V)	± 2σ	((^{206}Pb)/(^{204}Pb))	± 2σ	((^{208}Pb)/(^{204}Pb))	± 2σ	((^{207}Pb)/(^{206}Pb))	± 2σ	((^{208}Pb[1])/(^{232}Th))	± 2σ	((^{208}Pb$_{rad}$)/(^{232}Th))[2]	± 2σ	Slope	Age[1] (Ma)	Age[2] (Ma)	± 2σ
1	99SL-145_1	0.0043	0.7	1.39	0.8	65	5.9	628	6.1	0.1273	14.8	0.00405	0.8	0.00377	0.9	1.9528	41.9	39.0	0.9
2	99SL145_g	0.0005	3.7	0.10	2.0	23	8.0	75	6.4	0.3919	22.3	0.00558	3.3	0.00274	8.2	2.0145	55.9	27.4	2.3
3	99SL145_v	0.0021	1.5	0.66	1.6	39	17.3	392	12.1	0.2857	11.9	0.00420	1.2	0.00368	1.3	2.3520	36.1	31.6	0.7
4	99SL145_v	0.0022	2.0	0.76	2.4	47	10.8	452	9.2	0.2537	15.6	0.00384	1.3	0.00343	1.4	2.0145	38.5	34.4	0.8
5	An91C_j	0.0047	3.5	0.79	3.3	32	1.3	110	1.4	0.5032	1.4	0.00748	1.4	0.00492	1.2	2.3399	64.5	42.4	1.0
6	Bi9802b1	0.0021	5.2	0.64	3.7	123	2.4	124	2.7	0.1532	3.7	0.00467	1.9	0.00325	2.6	2.0145	46.8	32.6	1.1
7	Mo9804_w	0.0033	4.0	0.68	5.8	64	3.3	187	3.7	0.2351	4.9	0.00584	2.0	0.00472	1.7	2.3399	50.4	40.7	1.1
8	Po73_e	0.0032	1.8	0.86	1.7	140	4.3	230	4.3	0.1383	3.9	0.00495	1.0	0.00424	1.0	2.3399	42.8	36.6	0.8
9	Po73_r	0.0034	1.1	0.99	1.6	138	4.8	199	4.7	0.1220	4.0	0.00462	1.5	0.00380	1.2	2.3399	39.9	32.8	0.8
10	To81_r	0.0041	2.9	1.31	3.1	132	4.2	367	4.2	0.0980	5.3	0.00400	1.0	0.00358	1.0	2.3399	34.6	30.9	0.7
11	Tr92a_d	0.0033	9.8	0.52	10.2	26	2.2	86	2.7	0.5978	2.8	0.00940	3.4	0.00518	3.4	2.2578	83.9	46.4	1.8
12	Tr92_b	0.0049	2.5	1.34	1.5	49	2.3	178	2.2	0.3191	2.9	0.00491	1.3	0.00388	1.3	2.2578	43.9	34.7	0.8
13	Tr92_f	0.0080	4.5	2.05	4.4	83	3.1	275	3.0	0.2264	2.5	0.00512	1.5	0.00446	1.5	2.2578	45.8	39.9	1.0
14	Tr92_l	0.0053	1.7	1.44	1.7	53	1.8	219	1.8	0.2794	2.4	0.00485	0.8	0.00397	0.9	2.2578	43.4	35.5	0.8
15	Tr92_m	0.0030	2.6	0.70	3.3	44	3.3	125	3.2	0.3329	2.9	0.00530	1.7	0.00376	1.9	2.2578	47.4	33.6	0.9
16	Za75_j	0.0013	24.4	0.37	23.6	130	15.0	275	16.1	0.0872	57.3	0.00413	8.1	0.00297	14.6	1.9735	42.3	30.4	4.5
17	An91C_k in grt	0.0260	3.5	0.92	4.4	1258	7.0	3278	6.7	0.0642	1.6	0.03605	1.4	0.03591	1.5	2.1805	331.4	330.1	8.2
18	Pd79_1	0.0784	1.5	3.57	1.1	399	7.0	7809	7.1	0.0763	3.6	0.02902	0.8	0.02877	0.7	1.9528	298.1	295.6	6.3
19	PD79_j	0.0736	1.3	3.40	1.4	460	8.5	9992	8.6	0.0689	6.0	0.02819	0.8	0.02812	0.8	1.9528	289.7	289.0	6.2
20	PD79_n	0.0513	1.8	2.44	1.5	1174	6.6	6285	6.6	0.0587	1.7	0.02738	0.8	0.02719	0.7	1.9528	281.4	279.5	6.0
21	Ti81_g	0.0494	2.1	1.70	1.8	880	3.1	3140	3.1	0.0643	1.0	0.03843	1.4	0.03798	1.4	2.3399	329.2	325.4	7.9
22	Za72_l	0.0259	1.8	1.15	1.7	2602	7.2	4084	7.5	0.0541	1.0	0.02752	1.0	0.02727	1.0	2.1805	253.5	251.2	5.6
23	Za72_o	0.0368	2.0	1.61	2.2	1846	5.4	3559	4.1	0.0569	0.8	0.03005	1.1	0.02970	1.0	2.1805	276.7	273.4	6.2
24	Za72_p	0.0154	3.6	0.72	4.0	2089	9.2	3553	8.9	0.0563	1.5	0.02882	1.0	0.02846	1.0	2.1805	265.4	262.1	5.8
25	Za72_h	0.0209	1.4	0.98	1.7	1011	4.3	2222	4.3	0.0602	1.4	0.02778	0.7	0.02731	0.7	2.1805	255.9	251.6	5.3
26	Za75_h _zoned	0.0773	0.9	3.70	0.9	4507	10.0	16,109	10.0	0.0525	0.8	0.02645	0.7	0.02637	0.7	1.9735	269.1	268.3	5.7
27	Za75_s in grt	0.0254	2.4	1.04	2.6	1152	6.4	3705	6.5	0.0603	2.2	0.03164	0.8	0.03128	0.8	2.1805	291.2	287.9	6.2
28	Za75_t in grt	0.0344	2.5	1.60	2.6	474	4.8	1835	4.9	0.0791	2.3	0.02815	1.7	0.02744	1.6	2.1805	259.3	252.7	6.5
29	Za9705_B in grt	0.0298	9.1	1.42	9.1	775	6.9	2940	6.6	0.0629	3.6	0.02868	1.6	0.02818	1.6	2.0145	285.8	280.8	7.2
30	FC-1 std	0.0109	2.1	2.66	1.8	163	829.5	236	686.3	0.0477	1.5	0.00529	0.6	0.00525	0.7	1.9528	54.7	54.3	1.1
31	G7 std	0.3199	2.5	7.60	1.8	9584	34.2	69,530	34.2	0.0567	0.3	0.05649	1.0	0.05647	1.0	2.3399	482.2	482.0	10.8
32	G1A std	0.3594	1.4	7.22	1.2	3783	20.1	97,693	20.1	0.0601	0.8	0.06503	0.5	0.06511	0.5	2.3399	554.0	554.7	11.5

μ-XRF analysis: raw counts of Pb Lα, Th Ll, and U Ll used for age calculation (Cheburkin et al., 1997; Engi et al., this volume); EMP analysis: oxide wt.%'s of ThO_2, UO_2 and PbO required for age calculation (Montel et al., 1996; Scherrer et al., 2000); LA-PIMMS analysis: ages are calculated applying the formula: Age (years) = LN(1+(measured ratio ^{208}Pb/^{232}Th/Slope)) * 1/decay constant of ^{232}Th, where $\lambda = 4.9475e^{-11}$. The slope is calibrated by plotting LA-PIMMS measurements of HSA47, G1 and FC-1 for each session against their reference TIMS data (Parrish, personal communication).

valuable extra information on the growth topology relevant to heterogeneous monazite grains.
- An optical image of the grain mount provides information on which part of the grain has been successfully removed and whether the separate is clean or still contains other phases attached to it (potential interference).
- Combining all available information into a 'grain database'. This enables the interpretation of all information on age, composition, and structural context for each individual grain, and thus judge its geologic significance.

Once all the documentation is ready, monazite grains suitable for XRF-analysis, i.e. those not zoned in composition and preferentially larger than ~ 40 μm in diameter, can be drilled out and prepared for XRF-analysis. Following age determination by μ-XRF, the same grains may subsequently be analysed by an independent isotopic technique for higher precision, without substantial additional efforts being needed for sample preparation.

3. Performance of the XRF-microprobe and comparison with LA-PIMMS data

Chemical ages of monazite are mainly Pb/Th ages (see Montel et al., 1994). However, a direct comparison between isotopic $^{208}Pb/^{232}Th$ ages and chemical ages (Pb_{total}/Th_{total}) was missing so far. We used reference material monazite FC-1 derived from a pegmatite in the Canadian Cordillera (Parrish, 1995) to compare chemical dating with isotopic dating on single grains. Data for FC-1 are summarised in Tables 1 and 2. One large grain was characterised chemically by EMP analysis (for technical details refer to Scherrer et al., 2000), which confirmed a homogeneous large central part with relatively high Th contents. A narrow rim with slightly different Th and U contents surrounds the core. Pb contents are below the detection limit of the EMP, and thus, it is not possible to derive a chemical age by EMP. This is not so with the XRF-microprobe analysis with its considerably lower detection limit on Pb (10 ppm), which gives an apparent age of 55.3 ± 2 Ma.

The quality of the XRF data was assessed by other dating techniques, sequentially analysing several grains by EMP, XRF, and last by LA-PIMMS (Figs. 2–4; Tables 2 and 3). Comparing analyses made by the different technologies on standard FC-1 (Table 2; Fig. 2A), we measure a chemical XRF Th–U–Pb age (55.3 ± 2 Ma) that almost exactly matches the uncorrected (for ^{204}Pb) isotopic Th–Pb age by LA-PIMMS (55.2 ± 1.5 Ma). And both the corrected LA-PIMMS (54.4 ± 1.5 Ma) and the TIMS age (54.3 ± 1 Ma), upon which the former is based, are within the analytical uncertainty of the XRF-analysis (2σ). The LA-PIMMS technique involves a calibration that relies on TIMS analyses of three reference monazites encompassing different age brackets: monazite FC-1 at the lower end (54.3 Ma; Parrish 1995), monazite G1 from Madagascar (555 Ma; Paquette et al., 1994; Montel et al., 1996; Parrish, unpublished data, 1999), and monazite HSA47 (1880 Ma; Parrish, unpublished data, 1993). Each series of analyses is normalised to the slope, which is defined by plotting LA-PIMMS analyses of HSA47, G1, and FC-1 against their reference TIMS data (Table 3). The calibration of the XRF-microprobe relied on standards G1 (as above) and monazite G7 from Sri Lanka (460 Ma; Hansmann, unpublished data, 1996; Reusser, unpublished data, 1997; Scherrer et al., 2000).

Since XRF-analysis is nondestructive, there is no limit other than analytical efficiency as to how long a grain may be analysed. With cumulative acquisition measurements, the precision of an age determination can thus be optimised to a lower limit, from where it may no longer be economical. This is shown in Fig. 2A,B, displaying measurements of FC-1 at two different spatial resolutions in a series of equally spaced time intervals. Fig. 2A–D indicates the acquisition time necessary to date an individual grain separated from a polished thin section (approximate volume of 1.91×10^5 μm^3 with the 90 μm aperture and 0.34×10^5 μm^3 with the 38-μm aperture) to an uncertainty of ± 5% at the 2σ level. For example, 2 ng of Pb can be analysed at an accuracy of ± 9% (2σ) within 50-min integration time, which corresponds to a Pb concentration of ~ 200 ppm at a spatial resolution of Ø 90 μm (Fig. 2A). Relevant to smaller grains, 0.4 ng of Pb can be measured with an accuracy of ± 20% (2σ) within 150 min of integration time, which corresponds to a concentration of ~ 200 ppm Pb at a spatial resolution of 38 μm (Fig. 2B). The higher spatial resolution (38 versus 90 μm)

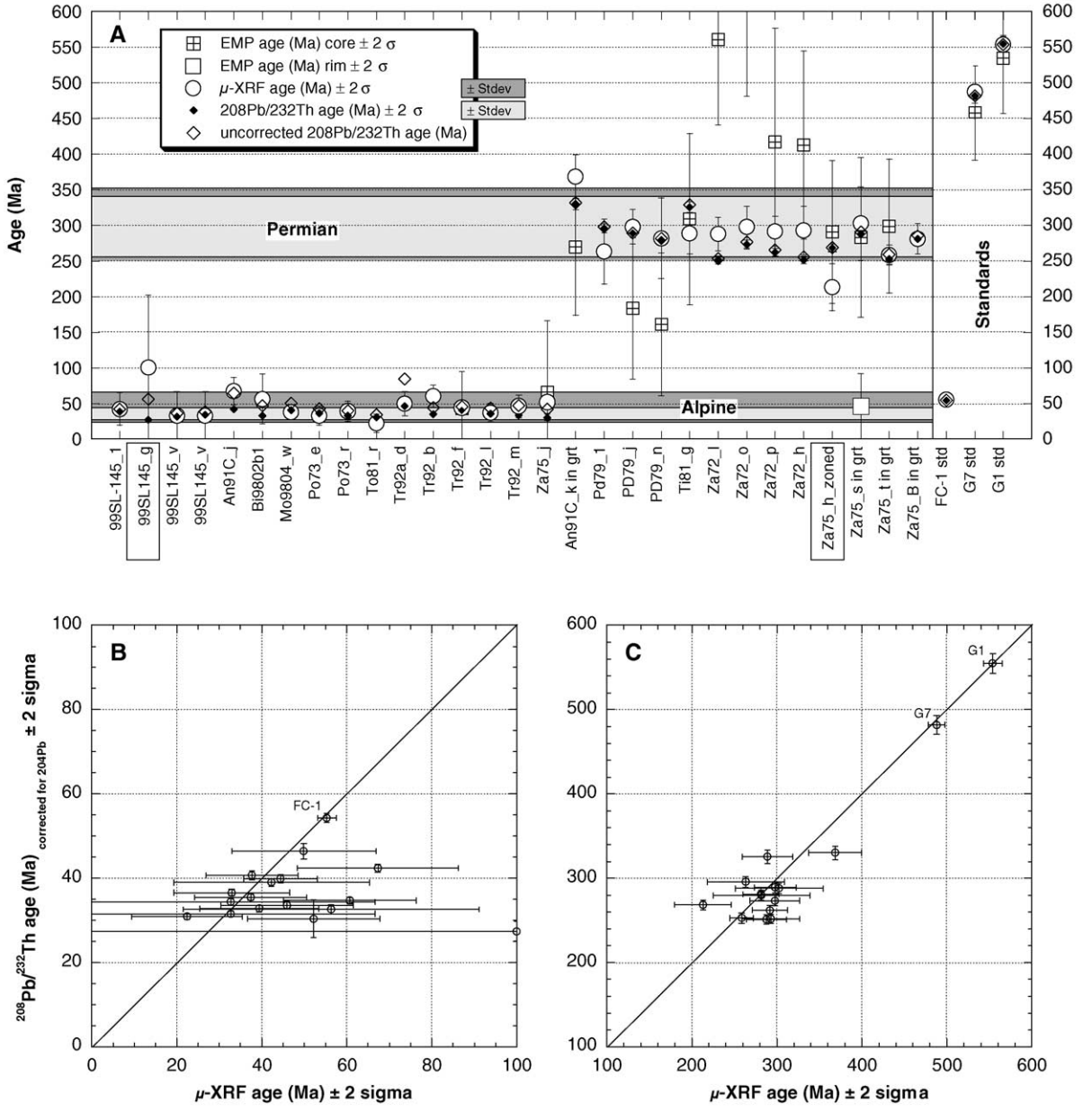

Fig. 3. Direct comparison of chemical Th–U–Pb ages (μ-XRF and EMP) with isotopic $^{208}Pb/^{232}Th$ ages (LA-PIMMS) for a set of sequentially dated, doubly polished, single grain separates ($n = 32$; refer to Table 3). Note that with few exceptions, integration time for the XRF analysis was generally 60 min and extended to a maximum of 120 min/grain, if < 100 Pb counts were accumulated in 60 min (compare Fig. 2). The grey shaded bands in (A) delimit one standard deviation about the mean of μ-XRF (dark) versus LA-PIMMS (light) analyses for the two populations (Alpine versus Permian). The two-boxed samples in (A) are discussed in the text. (B) and (C) present the same data as above, separated by age group, plotting chemical Th–U–Pb ages by μ-XRF against isotopically corrected $^{208}Pb/^{232}Th$ ages by LA-PIMMS. With young monazite (B), there is a tendency to an overestimation when applying chemical dating techniques (compare Fig. 4).

requires a nine- to ten-fold increase in integration time for the same level of precision. A choice is thus necessary between precise age data for a few grains (long integration times, repeated measurements) and reconnaissance age data for many grains (minimal integration times; e.g., cumulative acquisition only up to 100 Pb counts, accepting an individual uncertainty near $\pm 15\%$ in age at the 1σ level). The samples presented in Fig. 3 demonstrate that XRF ages are all within the 2σ analytical error of the isotopic age. Thus, relatively high-precision ages can be achieved using an XRF-microprobe, even for ages as young as Oligocene. The precision, however, depends on integration time as a function of grain size, Th-content, and age.

The age uncertainty is derived from the statistical uncertainty associated with the quantification of Pb ($N_{Pb}^{0.5}/N_{Pb}$), propagated to the age calculation. N_{Pb} signifies the total of counts accumulated on $Pb_{L\alpha}$. This seems to better account for variable volumes and integration times than the misfit error calculation outlined in Cheburkin et al. (1997), applied in earlier studies. No other correction is currently applied to the volume normalised primary data (Engi et al., this volume).

4. Discussion and conclusions

The new XRF-microprobe of the MPI Bern was specifically designed to lower the age limit for chemical Th–U–Pb dating of monazite, and improve the spatial resolution for this technique, which currently is below 40 μm. The original intention of in situ dating within Pb-free polished petrographic thin sections without destruction of the context could not strictly be achieved for reasons discussed earlier (penetration depth, interference). Nevertheless, the strategy, i.e. to be able to gain age information directly from a thin section, and thus interpret and discuss each monazite age within its original textural context, was still successfully applied with the presented methodology.

A very positive feature of the XRF-analysis is that no material is consumed by the analytical procedure. This has advantages over isotopic technologies:

- Precious standard material can be used indefinitely since it is not consumed upon analysis.
- Standardisation is therefore, not subject to age variations within a population of grains used as standard material, since one and the same standard grain can be used indefinitely.
- Small grains are not lost if an analysis fails for whatever reason—analyses can be repeated and cumulated many times.
- Verification of any XRF-analysis is possible by an independent isotopic technique (e.g., LA-PIMMS, TIMS, SHRIMP, SIMS).

A general disadvantage of a chemical dating technique is the lack of an isotopic correction for common lead. The current data set comprises 77 grains, of which 32 grains were successfully and sequentially analysed by both μ-XRF and LA-PIMMS (Table 3; Fig. 3). For grains of Permian age or older, such an isotopic correction (^{204}Pb) falls below 2% ($n=14$). Regarding age determinations of Tertiary monazite, an isotopic correction becomes more relevant. In the current data set, it ranges from below 2% to more than 50% and averages at about 25% ($n=16$). Thus, there is a tendency to an overestimation of Tertiary

Fig. 4. Assessing the influence of common Pb on chemical dating: Chemical Th–U–Pb dating of monazite makes the assumption that there is no initial Pb present in the mineral structure. The current data set presented in Fig. 3 and Table 3 are assessed by way of a box-plot, where each box encloses 50% of the data with the median value of the variable displayed as a line. Looking at chemical Th–U–Pb age determinations of Tertiary monazite, there is an increased chance to overestimate the 'true' age (A). Overall, common lead contents in monazite are indeed very low and do not significantly distort the age determination for ages older than ~ 200 Ma (B).

ages using XRF-analysis, tentatively quantified with a box plot in Fig. 4. The problem accentuates with very low Th contents (<0.5 wt.%, i.e. "99SL-145_g" of Fig. 3).

Because there is little or no control on the reliability of the achieved age with respect to the internal homogeneity of each grain, a combination of BSE images and EMP data compiled in a database, is used with the XRF-data. For example, insufficient spatial resolution leads to geologically meaningless analyses in chemically heterogenous grains, such as sample "Za75_h zoned" (Fig. 3). Here, the X-ray beam was too large to differentiate between the Permian and the Oligocene patches, which resulted in a 'mixed' age (circle, Fig. 3). This case demonstrates the advantage of using an electron microprobe (very high spatial resolution <5 μm) when analysing monazite from polymetamorphic rocks. Despite the 'reconnaissance' character of ages derived from quantitative analyses by electron microprobe (squares) for each chemically distinct zone, very useful information is gained, which may provide additional clues on the growth topology of each zone with respect to the microtextural context of a grain. At the same time, monazite growth ages may be linked to distinct P–T regimes of their microtextural context, as derived from EMP analyses of relevant mineral phases (Engi et al., 2001). Such an approach, as regarding the documentation of each single grain within its original context, is in any case well superior to bulk mineral separation techniques applied in conventional geochronology. Similar approaches have been presented in recent publications by Fletcher et al. (2000) and Terry et al. (2000), whereby a Sensitive High-Resolution Ion MicroProbe (SHRIMP) was applied for the age analysis. The volume resolution of a SHRIMP with spot sizes <10 μm is yet unmatched by Laser-ablation ICP-MS at comparable precision in isotopic ratio measurements (Fletcher et al., 2000).

A different approach is presented in an accompanying contribution (Engi et al., this volume), where large monazite populations (from classic mineral separates) were analysed by way of age distribution histograms to determine multiple growth phases of monazite within a rock sample. While these differing methodological approaches applying the XRF lead to cost-effective acquisition of age data well below the age limit of chemical dating by electron microprobe (100–200 Ma), there are limitations and disadvantages of the XRF in comparison with alternative

Table 4
This table summarises and compares several criteria to be considered when analysing monazite by any of the presented methods or a combination thereof

Criteria	EMPA	μ-XRF	LA-PIMMS
Th–U–Pb dating	chemical	chemical	isotopic
Common lead ^{204}Pb correction	no	no	yes
^{207}Pb/^{206}Pb ages	no	no	yes
Average precision at 2σ	±35%	<±10%	±1.5–5%
Spatial resolution	Ø<5 μm	Ø 38 or 90 μm	30×30 μm
Beam shape	spot or rectangle	fixed, circular	variable shape
Penetration depth	<5 μm	>1000 μm	~10 μm
Destruction during analysis	none	none	complete
Repeat measurement	possible	unlimited	not on same material
Optical control (real time)	very good	limited	good
BSE imaging (simultaneous)	yes	no	no
transmitted light (simultaneous)	yes	oblique	yes
reflected light (simultaneous)	yes	no	yes
beam visibility (simultaneous)	yes	no	yes
Average analysis time (min)	20	30–240	<5
Calibration time	3 h	–[a]	~30 min
stability of calibration	several days	–[a]	10–30 analyses
Consumption of standard material	small/unique	small/unique	considerable/continuous

[a] The μ-XRF calibration procedure involves a one-time effort at the initial set-up of the instrument. Thus, calibration time regarding μ-XRF analysis can essentially be neglected.

isotopic methods such as LA-PIMMS, ion microprobe, or single grain TIMS analysis:

- The lack of isotopic correction for common lead leads to slight overestimation of young ages, particularly with Th-poor monazite; overestimation, however, is within the 2σ uncertainty of the μ-XRF analysis for all the grains analysed in the present study.
- There are practical limits with respect to separating and handling very small grains. With training and experience, it is possible to drill out grains as small as 20 μm from a thin section.
- The method is not suitable to analyse small grains with heterogeneous age zones due to limited spatial and age resolution.

TIMS, LA-PIMMS (Parrish et al., 1999), SHRIMP (i.e., Fletcher et al., 2000; Terry et al., 2000), or Secondary Ionisation Mass Spectrometry (SIMS; Grove and Harrison, 1999; Catlos et al., 2000) analyses result in more accurate ages, but the equipment and laboratory operation are more costly and any material analysed, both standard and sample, is destroyed prior to/or during analysis. A comparison of several aspects to be considered is presented in Table 4. The level of age resolution combined with the high spatial resolution of an ion microprobe is yet unmatched by other techniques. Nevertheless, an XRF-microprobe permits acquisition of relatively precise ages down to Oligocene times using a low-technology method (low investment). The precision is sufficient to research complex polymetamorphic rocks (Engi et al., 2001), while the nondestructive nature of XRF-analysis does not exclude verification by a more precise isotopic dating technique using TIMS, LA-PIMMS, SHRIMP, or SIMS on grains that were already analysed by μ-XRF. In terms of advances in chemical Th–U–Pb dating of monazite, XRF-technology has significantly lowered the minimum age limit when compared with the electron microprobe.

Acknowledgements

This study was part of the first author's PhD thesis (http://www.earthsci.unibe.ch/people/scherrer/Thesis_PhD/PhD_Thesis_book.pdf) supported by Schweizerischer Nationalfonds (Credit 20-49671.96/1 and 20-55306.98/1). The EMP and XRF laboratories at the MPI Bern have been funded by Schweizerischer Nationalfonds (Credit 21-26579.89). Reviews by F. Finger, U. Schaltegger and an anonymous reviewer are gratefully acknowledged. **[EO]**

References

Catlos, E.J., Sorensen, S.S., Harrison, T.M., 2000. Th–Pb ion-microprobe dating of allanite. Am. Mineral. 85, 633–648.

Cheburkin, A.K., Frei, R., Shotyk, W., 1997. An energy-dispersive miniprobe multielement analyzer (EMMA) for direct analysis of trace elements and chemical age dating of single mineral grains. Chem. Geol. 135, 75–87.

Engi, M., Scherrer, N.C., Burri, T., 2001. Metamorphic evolution of pelitic rocks of the Monte Rosa nappe: constraints from petrology and single grain monazite age data. Schweiz. Mineral. Petrogr. Mitt. 81, 305–328.

Engi, M., Cheburkin, A., Köppel, V., 2002. Nondestructive chemical dating of young monazite using XRF: 1. Design of a miniprobe, age data for samples from the Central Alps, and comparison to U–Pb (TIMS) data. Chem. Geol. 191, 225–241 (this volume).

Finger, F., Broska, I., Roberts, M.P., Schermaier, A., 1998. Replacement of primary monazite by apatite–allanite–epidote coronas in an amphibolite facies granite gneiss from the eastern Alps. Am. Mineral. 83, 248–258.

Fletcher, I.R., Rasmussen, B., McNaughton, N.J., 2000. SHRIMP U–Pb geochronology of authigenic xenotime and its potential for dating sedimentary basins. Aust. J. Earth Sci. 47, 845–859.

Foster, G., Kinny, P., Vance, D., Prince, C., Harris, N., 2000. The significance of monazite U–Th–Pb age data in metamorphic assemblages; a combined study of monazite and garnet chronometry. Earth Planet. Sci. Lett. 181, 327–340.

Grove, M., Harrison, T.M., 1999. Monazite Th–Pb age depth profiling. Geology 27, 487–490.

Montel, J.M., Veschambre, M., Nicollet, C., 1994. Dating monazite with the electron microprobe. C. R. Acad. Sci. Paris II 318, 1489–1495.

Montel, J.M., Foret, S., Veschambre, M., Nicollet, C., Provost, A., 1996. Electron microprobe dating of monazite. Chem. Geol. 131, 37–53.

Montel, J.M., Kornprobst, J., Vielzeuf, D., 2000. Preservation of old U–Th–Pb ages in shielded monazite: example from the Beni Bousera Hercynian kinzigites (Morocco). J. Metamorph. Geol. 18, 335–342.

Paquette, J.L., Nedelec, A., Moine, B., Rakotondrazafy, M., 1994. U–Pb, single zircon Pb-evaporation, and Sm-Nd isotopic study of a granulite domain in SE Madagascar. J. Geol. 102, 523–538.

Parrish, R.R., 1990. U–Pb dating of monazite and its application to geological problems. Can. J. Earth Sci. 27, 1431–1450.

Parrish, R.R., 1995. Thermal evolution of the southeastern Canadian Cordillera. Can. J. Earth Sci. 32, 1618–1642.

Parrish, R.R., Nowell, G., Noble, S.R., Horstwood, M., Timmermann, H., Shaw, P., Bowen, I., 1999. LA-PIMMS: a new method

of U–Th–Pb geochronology using microsampling techniques. EUG10, Terra Abstr. 11, 799.

Rhede, D., Wendt, I., Forster, H.J., 1996. A three-dimensional method for calculating independent chemical U/Pb- and Th/Pb-ages of accessory minerals. Chem. Geol. 130, 247–253.

Scherrer, N.C., Engi, M., Gnos, E., Jakob, V., Liechti, A., 2000. Monazite analysis: from sample preparation to microprobe age dating and REE quantification. Schweiz. Min. Petrogr. Mitt. 80, 93–105.

Simpson, R.L., Parrish, R.R., Searle, M.P., Waters, D.J., 2000. Two episodes of monazite crystallization during metamorphism and crustal melting in the Everest region of the Nepalese Himalaya. Geology 28, 403–406.

Spear, F.S., Parrish, R.R., 1996. Petrology and cooling rates of the Valhalla complex, British Columbia, Canada. J. Petrol. 37, 733–765.

Suzuki, K., Adachi, M., 1991a. The chemical Th–U–total Pb isochron ages of zircon and monazite from the gray granite of the Hida Terrane, Japan. J. Earth Sci., Nagoya Univ. 38, 11–37.

Suzuki, K., Adachi, M., 1991b. Precambrian provenance and Silurian metamorphism of the Tsubonosawa Paragneiss in the South Kitakami Terrane, Northeast Japan, revealed by the chemical Th–U–total Pb isochron ages of monazite, zircon, and xenotime. Geochem. J. 25, 357–376.

Terry, M.P., Robinson, P., Hamilton, M.A., Jercinovic, M.J., 2000. Monazite geochronology of UHP and HP metamorphism, deformation, and exhumation, Nordoyane, Western Gneiss Region, Norway. Am. Mineral. 85, 1651–1664.